Received: 10 July 2024 | Revised: 14 September 2024 | Accepted: 23 September 2024

DOI: 10.1111/ijac.14959

International Journal of Applied Ceramic Technology

RESEARCH ARTICLE

Improving thermal insulation and thermal resistance properties of laterite-based geopolymer foams by direct foaming

Julson Aymard Tchio[1,2,3] | **Joelle Nadia Nouping Fekoua**[2,3] | **Cyriaque Rodrigue Kaze**[4] | **Juvenal Giogetti Deuton Nemaleu**[3] | **Juho Yliniemi**[1] | **Elie Kamseu**[2,3] | **Florence Uphie Chinje**[2] | **Cristina Leonelli**[5]

[1]Fibre and Particle Engineering, Faculty of Technology, University of Oulu Finland, Oulu, Finland

[2]Laboratory of Applied Inorganic Chemistry, Faculty of Science, University of Yaounde I, Yaounde, Cameroon

[3]Laboratory of Materials, Local Materials Promotion Authority, MINRESI/MIPROMALO, Yaounde, Cameroon

[4]School of Chemical Engineering and Mineral Industries (EGCIM) of the University of Ngaoundéré, Ngaoundéré, Cameroon

[5]Department of Engineering "Enzo Ferrari", University of Modena and Reggio Emilia, Modena, Italy

Correspondence
Julson Aymard Tchio, Fiber and Particle Engineering, Faculty of Technology, University of Oulu Finland, Oulu, Finland.
Email: Julson.tchio@oulu.fi and Julsontchio@yahoo.com

Funding information
Organization Internationale de la Francophonie; Organization of African, Caribbean, and Pacific States; European Commission, Grant/Award Number: FED/220/421-370; OEACP R&I, Grant/Award Number: PRICNAC-EEPER: MD2022

Abstract

This work aims to synthesize new foaming laterite geopolymer foam using laterite, sodium silicate solution, sand, and aluminium powder. The porosity rapidly increased with the addition of the foaming agent. The foam matrix had thermal conductivity values of 0.10 W/m K with 0.7% of Al powder and 0.64 W/m K with 0% of Al powder. For fire resistance, samples exposed to high temperatures (200°C and 500°C) showed increased flexural strength, linear shrinkage at 500°C, and a decrease at 900°C due to structural weakening under high thermal pressure and the appearance of new phases such as nepheline and akermanite in X-ray diffraction analysis. The results also showed that a 30% increase in fine aggregate content increased the strength of the foam matrix, with flexural strength ranging from 5 to 9.1 MPa after 28 days of ambient curing. These laterite geopolymer foams have shown promising thermal insulation and mechanical qualities that are appropriate for building applications.

KEYWORDS
geopolymers foam, laterite, thermal insulation, thermal resistance

1 | INTRODUCTION

Geopolymers, defined as inorganic polymers, have garnered significant attention over the last century due to their outstanding qualities.[1] These include: high thermal stability, strong thermal insulation, early high strength, low energy generation, low sintering production, low permeability, and good acid resistance.[2,3] The geopolymerization technique, discovered to be environmentally beneficial, sustainable, and energy efficient, involves dissolving raw aluminosilicate materials (such as metakaolin, fly ash, slag, etc.) in alkali hydroxide or silicate activation. This process generates aluminate and silicate species that link together during the polycondensation reaction. The resulting compact amorphous structure consists of alkali polysilicates, alkali ferrosilicate, and ferrisilicate.[4,5] Geopolymers are defined not only by the process conditions (curing time, temperature, and humidity) but also by the reactivity of the raw aluminosilicate. Reactivity is influenced by chemical and mineralogical composition, morphology, crystalline/amorphous content, and particle size distribution.[6] These versatile materials find applications in various disciplines, including thermal insulation, fire resistance, high-temperature engineering, geopolymer concrete for construction, building engineering, acoustic absorption, protective coating, and filtration.[6,7]

In recent years, significant advancements have been made in lightweight geopolymer composites, leading to the exploration of various fillers to enhance their mechanical, thermal, acoustic properties, and moisture absorption, thus expanding their applications in construction. Several types of fillers have already been utilized, ranging from natural and synthetic fibers to industrial by-products (metakaolin, fly ash, blast furnace slag, etc.),[8] lightweight aggregates (perlite, vermiculite, etc.),[9] and recycled materials (crushed glass and construction waste).[10] These fillers significantly influence the microstructure and properties of geopolymer foams (rheology, mechanical strength, linear shrinkage, thermal conductivity, etc.). For instance, Husainie et al.[11] demonstrated that the use of natural fibers instead of synthetic polyurethane improved tensile strength and thermal conductivity without significantly affecting the microstructure. Furthermore, Walbrück et al.[12] following the same approach, showed that fiber size and a proportion greater than 40% in a fly ash geopolymer foam impacts thermal conductivity due to a modification in the fiber–geopolymer foam interaction. The use of fine aggregates in porous geopolymers, on the other hand, increases pore size, thus promoting thermal conductivity while opposing a decrease in mechanical properties, as demonstrated by Abbas et al.[13] The judicious combination of fillers can lead to geopolymer composites with tailored properties suitable for specific applications, such as geopolymer concretes incorporating by-products or recycled products, which shows promise in reducing environmental impact while maintaining thermal insulation and mechanical properties significantly superior to those of ordinary Portland concrete; moreover, it demonstrated high corrosion resistance and long-term durability.[14–17] Thus, the combination of by-products and waste materials can lead to the formation of environmentally friendly porous geopolymers.

Geopolymer foam can be produced using a foaming agent (e.g., aluminum powder, hydrogen peroxide, or sodium perborate) or mechanical air pressure. Several investigations found that, increasing the foaming agent quantities reduces mechanical strength and density but increases porosity.[18,19] Szabó and Mucsi[20] created fly ash geopolymer foam with metallic powder and hydrogen peroxide, achieving compressive strengths ranging from 5.5 to 10.9 MPa and low thermal conductivity (0.11–0.39 W/m K). Vaou and Panias[21] observed similar results for perlite geopolymer foam (thermal conductivity: 0.03 W/m K), as did Kamseu et al.[22] for metakaolin geopolymer foam (thermal conductivity: 0.15–0.4 W/m K, porosity: 30%–70%). Controlling pore nature, size, and distribution is crucial for achieving desired properties in geopolymer foam. Smaller pores lead to lower air thermal conductivity.[23] The relationship between pore size and thermal conductivity in geopolymer foams is inverse; smaller pores result in lower air thermal conductivity.[18,19,24] This phenomenon can be observed across different pore size ranges, the air thermal conductivity of geopolymer foam with microcapillary pore ($\varphi \leq 50$ nm) is 0.002 W/m K, with microcapillary pore ($50\ \text{nm} \leq \varphi \leq 50\ \mu\text{m}$) it is 0.015 W/m K, and with $\varphi \geq 50\ \mu\text{m}$ it is 0.026 W/m K.[25] The water/solid ratio, temperature, the kind of alkali activator, the type of foaming agent, the type of raw material, the processing method, and the type of surfactant are characteristics that affect the pore microstructure (pore connectivity, porosity, and pose size distribution).[4,18]

Zenabou et al.[26] discovered that combining hydrogen peroxide and soluble silica produces porous geopolymers with nano, meso, and milliporosity. They explain that nano and meso porosity resulted from the substitution of rice husk ash on metakaolin while keeping the Si/Al ratio between 1.93 and 2.71. Adjusting the Si/Al ratio enhances heat conductivity in sponge geopolymer foam by improving connectedness, reducing porosity, and achieving a smaller pore size distribution.[27] Kamseu et al.[22] investigated the heat flux transport of sponge geopolymer foam and discovered that altering the mix design and amount of porogen resulted in the creation of capillary pores inside the matrix. The shape, geometrical distribution, and

connectivity of pores significantly influence heat flux transfer. However, other factors also play a role. For instance, the nonlinear relationship between tortuosity (path complexity) and both porosity and thermal conductivity affects heat transmission. Recent research has highlighted metakaolin and fly ash as primary solid precursors for designing and manufacturing porous matrices using the cold synthesis technique[23]; this process involves curing at low temperatures from 0°C to 70°C. Additionally, laterite (iron aluminosilicates) offers energy-saving benefits. Its main mineral, kaolinite, corrodes in the presence of iron. This reaction with silicon oxide and alkali solution allows for the creation of various levels of porosity.

The objective of this study is to synthesize laterite geopolymer foam using aluminium powder as a foaming agent via a cold sintering process (curing at low temperatures). We will investigate the impact of fine aggregate and the foaming agent on pore structure, thermal conductivity, pore size distribution, and thermal resistance of the geopolymers.

2 | MATERIALS AND METHODS

2.1 | Materials

The geopolymer binder was prepared using iron-rich laterite as a solid precursor (Montée des Soeurs) with partial substitution of fine sand aggregate (Razel). The chemical composition of fine aggregate was determined previously by Kaze et al.[28] X-ray fluorescence of laterite was done in the previous study by Tchio et al.[6] Laterite and fine aggregates were ground and sieved below 100 μm. The alkaline activator used was a local sodium silicate solution, which was prepared using biomass source SiO_2 (rice husk ash [RHA]), NaOH pellets (98% purity, Sigma–Aldrich) and water with the following characteristics: molar ratio $(SiO_2/Na_2O) = 2$ and $(H_2O/Na_2O) = 10$. The foaming agent was aluminum powder from Germany (Art-No. 5285.2) with a particle size under 50 μm.

2.2 | Methods

Due to the lack of standards available for geopolymer foam, several geopolymer foam and Portland cement foam concrete specifications have been used as a starting point.[2,16] The laterite and fine aggregate were dry mixed for 5 min, followed by the addition of sodium silicate solution. The geopolymer paste was mixed with a rotative mixer for 6 min then aluminium powder was added to the homogeneous geopolymer paste and the final mixture was done in 3 min (the mix design are illustrated in Table 1). Low-speed mixing was used to avoid bubble breakage due to the high viscosity of the geopolymer paste. The final foamed mixtures were poured into 4 × 4 × 2 mm plastic molds, cured at 70°C for 24 h, demolded and sealed into a plastic paper for 28 days at ambient conditions, till mechanical and physical properties and other characterizations were carried out. The choice of solution/solid radio was chosen based on the works of Ibrahim et al.[29] that showed the influence of liquid/solid ratio on lightweight geopolymers. Al powder used in percentage of mass of laterite varying from 0.2% to 1% as inferred from the literature on metakaolin geopolymers foam.[30]

2.3 | Characterization methods

2.3.1 | Mechanical testing

The flexural strength of the laterite geopolymers foam (LGF) was tested using an Instron 1995 mechanical testing machine with a displacement of 4 mm/min. A total of three specimens were tested, and the average result was presented. A slight volume change after curing was noted; therefore, the top surfaces of the samples were carefully sanded to make them flat and parallel prior to testing. The diameter and length of each sample were measured to calculate the demold density (volume). The dry density of LGF was also measured after drying the pulverized samples in an oven at 70 ± 2°C for 24 h according to ASTM C495. For intensity and density measurements, the average of three samples for each mixture is reported, and the standard deviation for each mixture is reported as a significant error.

2.3.2 | Mercury intrusion porosimetry

Pieces collected from different formulations after the three-point bending test were used to prepare specimens for the MIP (Auto Pore IV 9500 V1.09) tests using one high-pressure analysis port (33 000 psia maximum pressure) and two low-pressure analysis ports. Each specimen was put in a penetrometer with 15 mL sample cup and steam volume of 1.1 mL (the steam volume depends on the penetrometer used for this study used one with steam volume of 1.1). The total pore volume was evaluated using the set-time equilibrium (10 s) mode between pressure limits of 345 kPa and 228 MPa covering the pore diameter range from approximately 0.0055 to 360 μm.

2.3.3 | Thermal conductivity

The thermal conductivity of LGF was measured at ambient conditions using the transien plane source (TPS) method

TABLE 1 Mix design of laterite geopolymer foam (LFA_iF_j, where "*i*" represents the proportion of fine aggregate and "*j*" represents the proportion of aluminium powder in percent).

Mixture	Laterite (g)	Fine aggregate (g)	Solution/solid	Foam dosage (%)
LFA_0F-0.6	400	0	0.4	0.6
$LFA_{10}F$-0.6	360	40	0.4	0.6
$LFA_{20}F$-0.6	320	80	0.4	0.6
$LFA_{30}F$-0.6	280	120	0.4	0.6
$LFA_{40}F$-0.6	240	160	0.4	0.6
$LFA_{50}F$-0.6	200	200	0.4	0.6
$LFA_{30}F$-1	280	120	0.4	1
$LFA_{30}F$-0.8	280	120	0.4	0.8
$LFA_{30}F$-0.7	280	120	0.4	0.7
$LFA_{30}F$-0.5	280	120	0.4	0.5
$LFA_{30}F$-0.4	280	120	0.4	0.4
$LFA_{30}F$-0.2	280	120	0.4	0.2
$LFA_{30}F$-0	280	120	0.4	0

Note: "g" represents the proportion in grams.
Abbreviations: FA, fine aggregate; L, laterite.

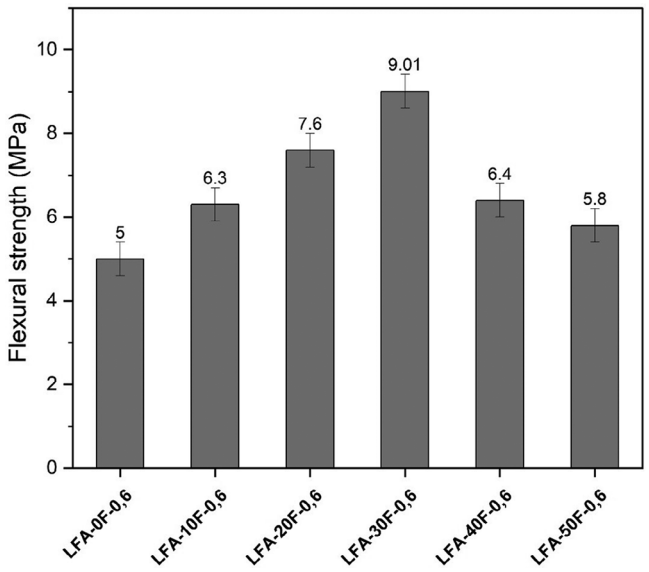

FIGURE 1 Flexural strength of laterite geopolymers foam (LGF) substituted with fine aggregate.

on a Hot Disk 2500 SYSTEM. The samples were cut from the LGC specimens with 4 × 2 mm to form a square with a thickness of 2 mm. To ensure good contact between the TPS element and the sample surface, all samples were polished flat and parallel, and cleaned with compressed air. For each LGC foam mixture, tree replicate tests were conducted.

According to Zhang et al.,[27] the humidity of the sample has an important impact on the measured thermal conductivity. Because drying for a long period may impact the microstructure/phases of LGF. A short period of drying (24 h) at low temperatures was adopted in this study. Further samples dried for more than 24 h showed that the weight loss and shrinkage did not exceed 1%. The fast drying at the temperature of 70°C is due to the porous microstructure and low thickness.

2.3.4 | Thermal resistance and optical microscope

The thermal resistance of LGF was evaluated by measuring the change in strength and volume after exposure to high temperatures. Selected samples were heated from room temperature to 200°C, 500°C, and 900°C in a programable electric furnace with a thermal treatment rate of 5°C/min (ISUNI, type MN 51 A) for 3 h, then cooled at room temperature in the furnace. Test of flexural strength of LGCF before and heating using Instron 1995 mechanical testing machine with a displacement of 4 mm/min, a total of three specimens was tested and the average result was presented. The linear shrinkage of the heated samples was also measured. The microscopic images at the cross-section of the samples were captured using a 3R-MSUSB401 optical microscope produced by Anyty. Then, the magnitudes of roundness and pore size were determined by processing the image through an image analysis software (image pro plus 6.0).

2.3.5 | Structural analysis

Phase evolution transition after heating analysis by X-ray diffraction (XRD) was done using a PANalytical copper pro diffractometer (Bruker) with a copper target

$\lambda K\alpha 1$ = 1.5405 Å. The working conditions of the diffractometer were 40 kV and 40 mA. Measurements were made from 2° to 70°, 2θ at the rate of 10°/min with a step size of 0.02° 2θ. FTIR (Fourier Transform Infrared Spectroscopy) was performed using a NICOLET 6700 FTIR series averaging spectrophotometer in attenuated total reflection mode with diamond crystals. The infrared spectra were digitally recorded in the 4000–500 cm^{-1} range using finely ground and sieved powders at 100 μm. The water absorption and the bulk density were carried out using the Archimedes method according to ASTCM. These measurements were carried out according to the Archimedes method using an electric balance with a sensitivity of ±0.001 g.

3 | RESULTS AND DISCUSSION

3.1 | Characterization before fire resistance

3.1.1 | Effect of fine aggregate addition on flexural strength

The effect of fine aggregate on the flexural strength of LGF is depicted in Figure 1 at the constant foam dose of 0.6% of aluminium powder; this proportion was selected according to the study of Zhang et al.[2] and Arrasi.[30] Without fine aggregate added to laterite, the flexural strength was 3.25 MPa after 28 days of testing. By increasing the fraction of fine aggregate up to 30%, the flexural strength was 7.6 MPa. Further substitution reduces the mechanical properties of LGF. In fact, due to the geopolymerization action between laterite, fine aggregate, and RHA sodium silicate solution. This will lead to an improvement of certain properties (flexural strength) of the LGF. Fine aggregate substitution into laterite influences the pore structure and mechanical properties of the resulting geopolymer foam due to the rheology and fast setting time. The increase of strength when incorporating fine aggregate up to 20% is due to the fact that the amount of particles was not enough for the foam expansion and pore structuration organization. As shown in Figure 1, 30% substitution is the appropriate fine aggregate concentration for balancing pore structure and mechanical strength. Furthermore, the performance may be attributed to the alkaline solution, which permitted the high dissolution of iron aluminosilicate (laterite) and aluminate, silica, resulting in the production of porous and strong matrix, ensuring higher strength and rigidity. Further incorporation of fine aggregate (at 40% and 50%) reduces matrix strength, which can be explained by (1) saturation of the entire system with Si and Al species from replaced fine particles. Those materials that were not integrated into the LGF would have compromised its strength. (2) Additionally, higher fine aggregate content tends to reduce the porosity and density of the LGF. (3) Furthermore, due to the reduced strength, finer aggregate will not provide nucleation sites for air bubbles to foam.

3.1.2 | Effect of aluminium powder addition on flexural strength and bulk density

Based on the previous results, Figure 2a illustrates the impact of aluminium powder on the LGF with 30% fine aggregate substitution. Adding 0.2% of foaming agent increased the matrix flexural strength to 13 MPa. At low concentrations of aluminum, a lesser amount of hydrogen is expected to be released, resulting in higher densities. A similar trend was observed in the density of the LGF matrix, where the addition of foaming agent raised the density from 1703 to 1823 kg/m^3, as depicted in Figure 2b. This increase can be attributed to the influence of the foaming agent on foam density and cell structure. Studies by Beghoura and Castro-Gomes[31] and Ducman and Korat[32] reported similar findings in Portland foam concrete and fly ash–geopolymers foam. However, increasing the aluminum powder dosage from 0.3% to 1% reduced the strength and density of the samples. This could be explained by (1) the formation of a more extensive porous structure with larger pore sizes, leading to interconnected pores compared to non-foamed LGF. (2) Additionally, the thinning of pore walls due to the foaming agent resulted in an open-cell foam network with large macropores. This is unfavorable for foam geopolymer as it diminishes the material's resistance to chemical and water penetration and its lightweight density. Compared to fly ash-slag geopolymer foams,[33] geopolymer foam concrete,[32] and Portland concrete foam,[34] with strength and density ranging 2–18 MPa, 1.10–8.13 MPa, and 1–40 MPa and 650–1224 kg/m^3, 800–2000 kg/m^3, and 400–1200 kg/cm^3, LGF exhibits higher flexural strength and an average density ranging from 1000 to 1800 kg/m^3. When comparing the results to those of older studies,[2,10,14,35,36] it must be pointed out that the geopolymer foams based on laterite exhibit higher mechanical strength and slightly higher density compared to foams prepared with metakaolin, fly ash, red mud, and Portland cement, which generally have a flexural strength ranging from 1 to 10 MPa and a density ranging from 360 to 1400 kg/m^3. Therefore, it can be inferred that LGF has a variety of applications from semi-structural to structural due to its high strength and density.

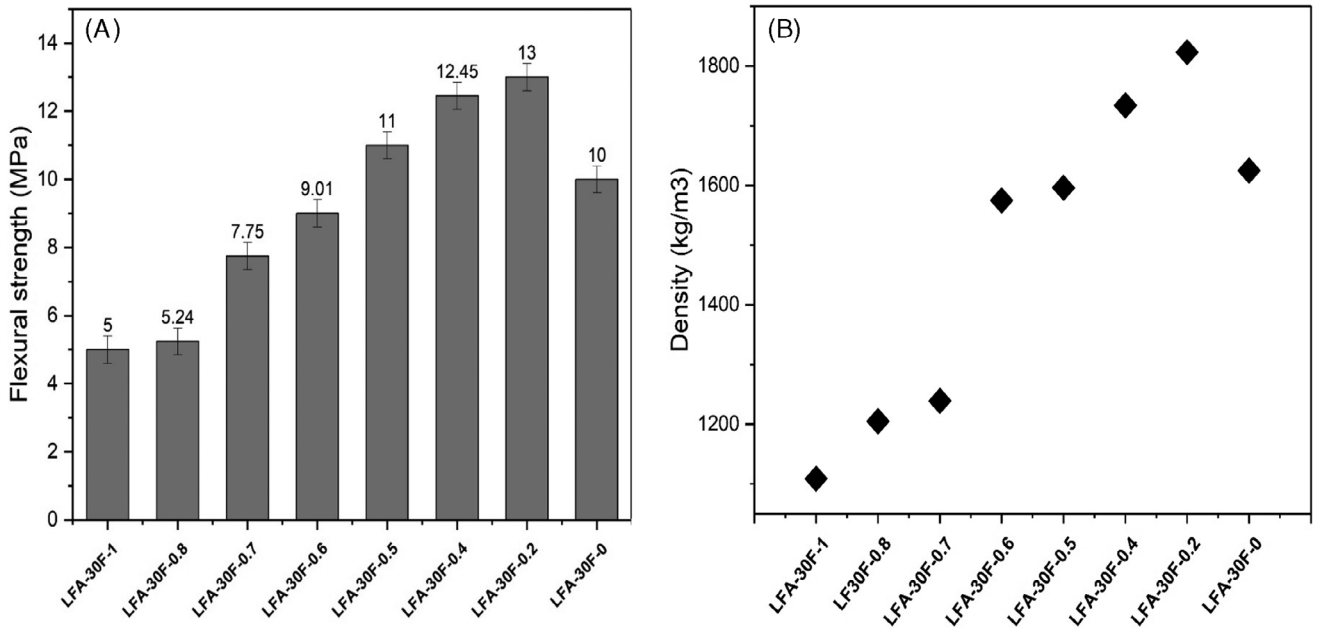

FIGURE 2 (a) Flexural strength and (b) bulk density of laterite geopolymers foam (LGF) substituted with different proportion of Al powder.

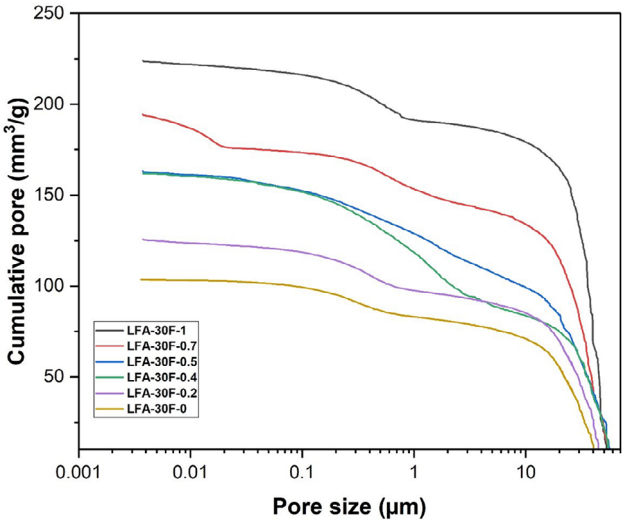

FIGURE 3 Mercury intrusion porosimetry of laterite geopolymers foam (LGF) with different percentage of foaming agent.

3.1.3 | Mercury intrusion porosimetry

Figure 3 illustrates the variation in cumulative pore volume of LGF composite specimens labeled $LFA_{30}F$-0, $LFA_{30}F$-0.2, $LFA_{30}F$-0.4, $LFA_{30}F$-0.5, $LFA_{30}F$-0.7, and $LFA_{30}F$-1 of Al powder. The values recorded are 119, 123, 155, 155, 185, and 220 mm^3/g for $LFA_{30}F$-0, $LFA_{30}F$-0.2 g, $LFA_{30}F$-0.4, $LFA_{30}F$-0.5, and $LFA_{30}F$-0.7, respectively. The addition of Al powder notably increases the cumulative pore volume, as observed in Figure 3. This trend is likely attributed to the reaction between the Al powder and alkaline solution, releasing H_2 that creates pores within the structure.

$$Al + 3H_2O + OH^- \rightarrow [Al(OH)_4]^- + H_2$$

These findings align with the flexural strength results, indicating that a higher quantity of Al powders results in larger pores that compromise the material's strength. This result ties well with the previous study done by Masi et al.[37] on Fly ash foam wherein the pore size distributions shows similar trend for all the different sample foamed with the concentration of aluminium powder and hydrogen peroxide. However, its cumulative pore volume ranged from 300 to 400 mm^3/g, whereas in this case, it ranges from 100 to 225 mm^3/g. This suggests that the geopolymerization reaction of iron-rich laterite is significantly different from that of fly ash geopolymers. The emergence of pores suggests that the addition of Al powder enhances the formation of insulating materials, characterized by open voids, capillary pores, and meso-pores. Previous studies have demonstrated that during the polymerization of laterite without a pore-forming agent, mesopores are formed in the matrix due to the reaction of iron with the alkaline solution and silica, providing insulating properties as reported in earlier research.[5,6]

3.1.4 | Thermal conductivity and optical microscopy

The finding from Figure 4 demonstrates the decrease of thermal conductivity up to $LFA_{30}F$-0.7 (0.10 W/m K) and

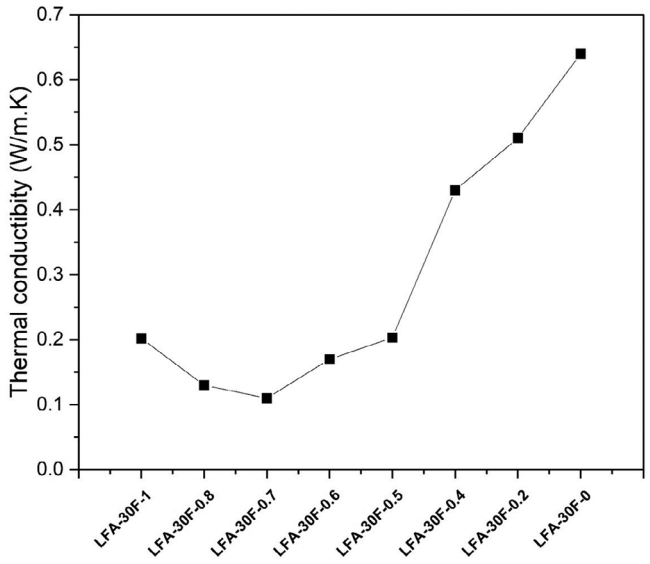

FIGURE 4 Thermal conductivity of laterite geopolymers foam (LGF).

then an increase in thermal conductivity with decreasing amount of aluminium powder supporting the theory that porosity has a significant role in influencing the thermal conductivity of porous materials. This implies that conductivity is impacted by the pores found in LGF. The interior structure of LGF contains low-thermal conductivity air molecules that contribute to both the lowering of thermal conductivity and the speed of propagation. On samples $LFA_{30}F$-0.8 and $LFA_{30}F$-0.7 (0.13 and 0.10 W/m K), the drop in thermal conductivity attempts to stabilize, but it increases in LGF-0.6 (0.1703 W/m K). The poor conductivity of 0.10–0.13 W/m K can be explained by the close porosity of $LFA_{30}F$-0.7 and $LFA_{30}F$-0.8, which results in low gas circulation in pores and weakens heat transmission by radiation between pore walls. For samples ranging from $LFA_{30}F$-0.5 to $LFA_{30}F$-0, the increase in thermal conductivity is due to a progressive decrease in porosity. Because due to the lack of pores, air molecules can quickly rise in conductivity, which contributes to the increase in conductivity. Therefore, the conductivity of LGF and others geopolymers foam is mainly a function of the proportion solid and air with are currently illustrated by the total porosity. Similar findings were made by Yan et al.[38] who used red mud/slag-based materials to create porous geopolymers. They even confirmed that the flexural strength increases with decreasing pore size and decreases with increasing thermal conductivity, which supports the findings in the preceding section.[38,39] The thermal conductivity of porous Portland concretes ranges between 0.3 and 0.5 W/m K,[25] and for LGF, it ranges between 0.10 and 0.5 W/m K. Comparing the thermal conductivity results for fly ash foam, metakaolin foam, and fly ash/slag foam reported by Xu et al.,[40] Bai et al.,[41] and Wu et al.[42] to those of lightweight geopolymer foam, significant similarities were observed within the thermal conductivity range of 0.095–0.5 W/m K. It is crucial to emphasize that curing conditions and the type of foaming agent exert varying influences on thermal conductivity. Zhang et al.[2] discovered that curing geopolymer foams at 80°C results in enhanced insulation properties. Notably, previous research has predominantly focused on utilizing various industrial by-products for the synthesis of foam insulation materials, while laterite remains largely unexplored in this context. Due to its low thermal conductivity, iron-rich laterite can be regarded as an excellent material for manufacturing building thermal insulation panels. Through the course of this experiment, we were able to evaluate how the performing agent affected the mechanical characteristics, pore dispersion, and thermal conductivity of the laterites incorporating the fine aggregate powders.

The LGF foams were examined using a high-resolution optical microscope to evaluate the samples porosity and provide an overview of the pore size distribution. Figure 5 illustrates images of selected LGF samples: (a) LFA30F-1, (b) LFA30F-0.7, (c) LFA30F-0.6, and (d) LFA30F-0.2. A decrease in the proportion of foaming agents leads to a reduction in the number of pores and, consequently, the overall pore volume. Correspondingly, the pore size tends to decrease. This observation aligns with the fact that reducing the foaming agent results in higher density and compressive strength. The shape of the pores appears irregular, even when varying the aluminum content. This irregularity is possibly due to the more intense conditions of gaseous hydrogen release, leading to variations in cumulative pore volume and pore size. Overall, the development of geopolymer foams using laterite as a precursor is a relatively new field. Limited information is available regarding the relationship between the composition, structure, and properties of these new materials.

3.2 | Characterization after thermal resistance tests

3.2.1 | Mechanical properties after thermal exposure at high temperatures

The flexural strength values of LGF with 30% fine aggregate are depicted in Figure 6 after exposure to temperatures ranging from 200°C to 900°C. This assessment of LGF thermal resistance involves monitoring changes in volume and strength following exposure to high temperatures. Samples exposed to 500°C exhibited increased strength regardless of the amount of foaming agent incorporated

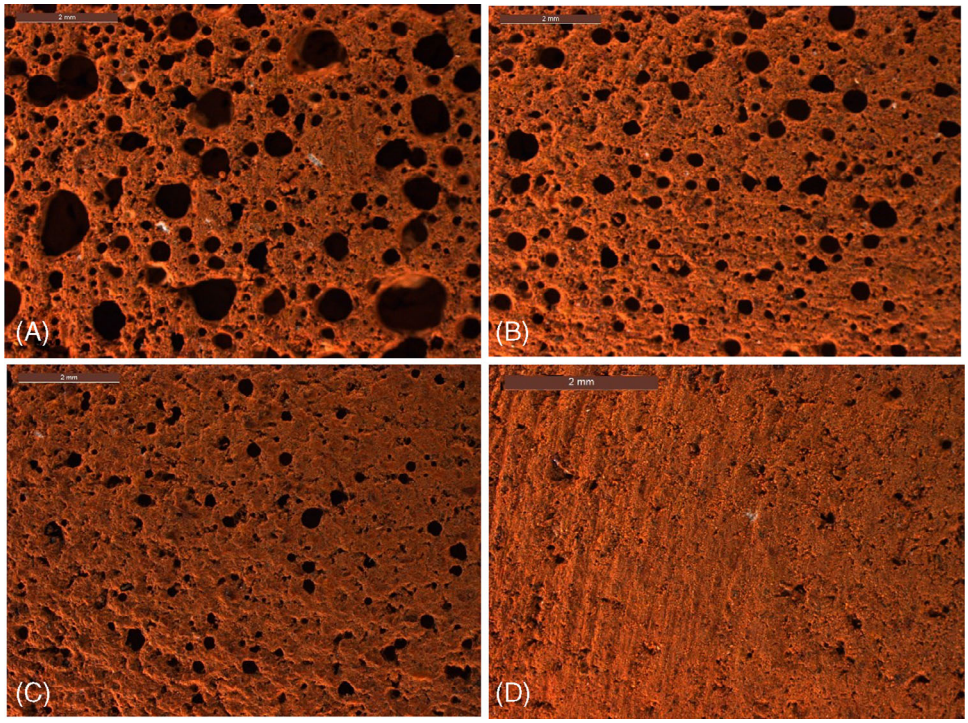

FIGURE 5 Optical microscope of laterite geopolymers foam (LGF): (a) LFA30F-1, (b) LFA30F-0.7, (c) LFA30F-0.6, and (d) LFA30F-0.2.

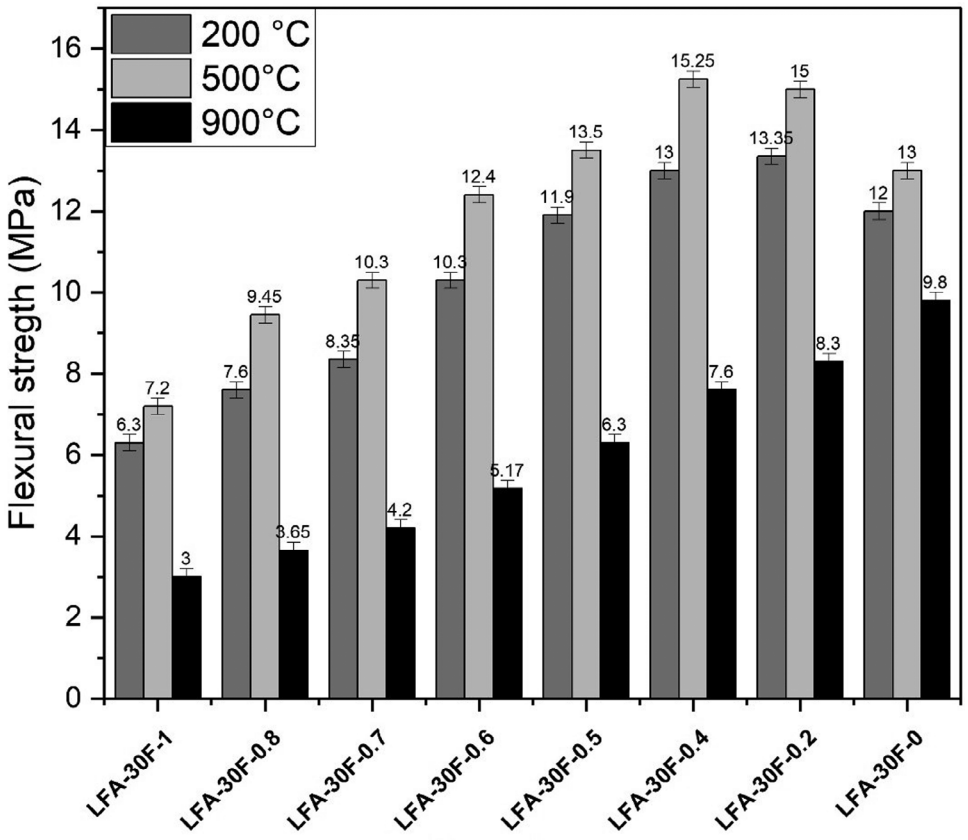

FIGURE 6 Flexural strength of laterite geopolymers foam (LGF) after exposure at different temperatures.

into the matrix (10.3 MPa at 500°C for sample $LFA_{30}F$-0.7). However, samples exposed to 200°C and 900°C showed a decrease in flexural strength. The strength increase at 500°C can be attributed to several factors: (1) crystallization of remnant amorphous phases such as kaolinite, gibbsite quartz, and goethite,[27] (2) improved fritting and densification at 500°C leading to mechanical consolidation, and (3) partial disintegration of compounds at 500°C that may have been stable at 200°C. These findings align with research on fly ash-based geopolymer insulation by Krzywon et al.,[43] where fly ash strengthened when exposed to a pore-forming chemical at 400°C. Le et al.[44] studied the fire resistance of metakaolin with a foam layer of polystyrene and found that chemical bond stability was achieved between 500°C and 600°C, consistent with the LGF results. The pressure inside the pore counteracts thermal expansion at 500°C, aiding in stabilizing the structure. Additionally, the residual strength of LGF after exposing at elevated temperatures is mainly influenced by the gel composition (Fe–Si–Al gel) from iron-rich laterite, in the case of metakaolin, and fly ash on the other hand, the Al–Si gel influence the strength as found Dhasindrakrishna et al.[14] Due to the high chemical bound water in geopolymers gel (Ca-rich gel) made from slag, exposing it at the same temperature will destroys the Ca-rich gel.[45]

Le et al.[18] demonstrated the maximum temperature for geopolymer insulation foam, which varies based on raw material composition and activating solution type. However, this study reveals a 50% decrease in flexural strength at 900°C regardless of the amount of Al powder incorporated. Notably, there was approximately a 30% decline between $LFA_{30}F$-0 and the other samples containing the pore-forming agent. This decrease is typically due to disruption in the loss of chemically linked water and destabilization of the pore structure caused by bond rupture in the matrix.

He et al.[46] previously showed that the strength decrease in fly ash substituted with steel waste at high temperatures was due to poor intergranular connectivity and unreacted fly ash, consistent with the current findings. At 500°C, the LGF structure remains dense and solid despite pressure on porous walls, while at 900°C, thermal stresses cause fragilization of porous paths, cracks on specimen surfaces, and eventual collapse. The difference in flexural strength between LGF without and with a pore-forming agent is also influenced by changes in physical and mechanical parameters such as matrix volume, pore structure, and phase decomposition. Compared to $LFA_{30}F$-0, the volume shift did not result in surface cracks, explaining the limited strength loss. Notably, subjecting a porous geopolymer to high temperatures such as 900°C leads to crack formation through a stochastic process, resulting in cracks of varying diameters in each sample and loss of characteristics, consistent with findings from other studies.[46–48]

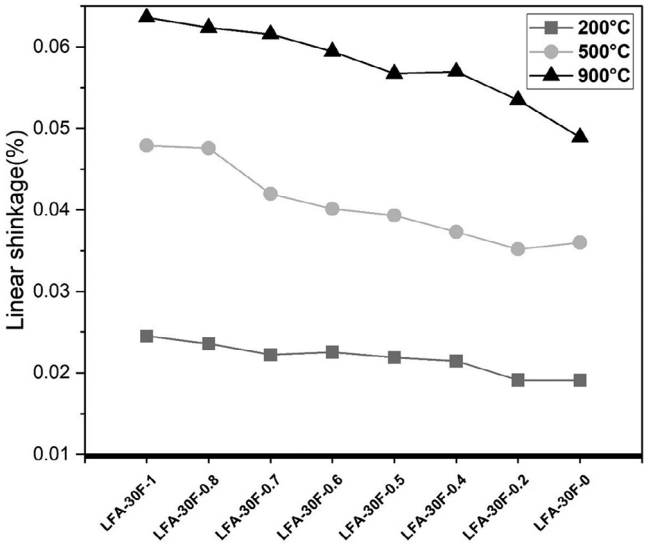

FIGURE 7 Linear shrinkage of laterite geopolymers foam (LGF) after exposure at different temperatures.

3.2.2 | Linear shrinkage after exposure at elevated temperature

Figure 7 illustrates the volumetric stability, expressed in terms of linear shrinkage, of LGF after exposure to varying temperatures. It was observed that linear shrinkage increases proportionally with the temperature within the studied temperature range, as dimensional measurements are taken after the samples have cooled. From room temperature to 200°C, the linear shrinkage of the samples ranged between 0.024% and 0.019% following exposure to temperature. As the proportion of the pore-forming agent decreased, the linear shrinkage also decreased. In the temperature range of 45°C–300°C, the evaporation of free water is a commonly observed phenomenon in porous geopolymer matrices. Studies by Kuenzel et al.[49] have shown that under similar temperature conditions, the evaporation of free water can lead to crack formation on the surface of metakaolin geopolymer samples and, at times, high linear shrinkage. Similarly, Cheng-Yong et al.[50] demonstrated that exposure to temperatures below 200°C resulted in low linear shrinkage for fly ash. Due to the low density of LGF, there were no signs of expansion after cooling to ambient temperature. This observation aligns with findings by Zhang et al.[27] during the production of porous geopolymers using oxygenated water. Contrary to these observations, Provis et al.[51] demonstrated that the dilatometric expansion of a geopolymer gel could be below 250°C. However, it is important to note that dilatometric

studies are typically conducted at high temperatures and often result in minimal overall dilation when water retraction occurs.

Upon exposure to temperatures of 500°C and 900°C, linear shrinkage was observed in the sample dimensions. At 500°C, the increase in linear shrinkage can be attributed to the loss of hydroxide molecules bound in the porous geopolymer matrix, as well as the decomposition and oxidation of any remaining unreacted aluminum powder, leading to gas release and volumetric contraction. This phenomenon can also be explained by the transformation of amorphous crystalline phases, typically following the crystallization of sodium aluminosilicate. The evaporation of residual free water, coupled with the progressive dehydroxylation of N–A–S–H, ferrosilicate, and ferrisilicate gels, results in significant volumetric and linear dimensional shrinkage of the structure. Prior studies by Kamseu et al.[5] and Tchio et al.[6] have shown that the evolving polymerization of iron aluminosilicates leads to a modification of interparticle attractive forces, enhancing the obtained flexural strength results. A linear shrinkage ranging from 0.05% to 0.06% was observed when the samples were exposed to a temperature of 900°C. The linear shrinkage analysis revealed that laterite-based geopolymer foams exhibited significantly enhanced shrinkage resistance compared to their fly ash- and metakaolin-based geopolymer foams where a notable linear shrinkage of 0.13% was observed at the temperature range of 800°C–1000°C. This phenomenon can be attributed to viscous sintering effects. During the process of viscous sintering, the porous geopolymer gel undergoes a transformation into a more mobile viscous phase. This increased mobility enables the material to infiltrate and occupy pore spaces, consequently leading to an increase in linear shrinkage.[2,40,41,45,52] The linear shrinkage reduction of LGF compared to other temperatures is attributed to the complete decomposition of aluminum and iron-rich Fe–N–A–S–H formed during polymerization, resulting in a progressive breakage of the Al–O–T (Al, Si, Fe) bonds. At such temperatures, sintering phenomena are more commonly observed, characterized by significant linear shrinkage. He et al.[46] have demonstrated that when all porous geopolymer components are subjected to temperatures between 700°C and 900°C with an increasing heating rate, softening and vitreous sintering of aluminosilicate gels occur, leading to densification into a glassy state. Additionally, Zhang et al.[27] have shown that an increase in the SiO_2/Na_2O ratio can decrease the sintering point from over 1000°C to 700°C for a solid–liquid ratio of 0.125 when the SiO_2/Na_2O ratio increases from 0 to 0.2. Moreover, a higher solid–liquid ratio can lead to an increase in the sintering point.

3.2.3 | Water absorption and bulk density after exposure to elevated temperature

Water absorption rate and apparent bulk density after exposure to varying temperatures (16.56% and 1.82 g/cm^3 at 200°C; 14.67% and 1.66 g/cm^3 at 500°C; 29.46% and 1.17 g/cm^3 at 900°C) are illustrated in Figure 8. It was observed that the water absorption rate at 200°C was slightly higher compared to that at 500°C; conversely, the apparent bulk density exhibited the opposite trend. This difference may be attributed to the less stable structure of the porous geopolymer material at 200°C, resulting from the inactivation of chemical transformations of unstable compounds within the matrix (such as the conversion of goethite into hematite, absence of transition from alpha quartz to beta quartz, and presence of kaolinite, iron silicate, and ferrosilicate phases).

At 500°C, the water absorption rate decreased due to the presence of a stable porous structure with closed pores, leading to a reduced absorption rate. This decline can be linked to a complete transformation of oxides and unstable compounds within the structure, as well as an improved organization of the crystalline network of the porous LGF. However, as the temperature rise to 900°C, structural weakening occurred due to high linear shrinkage and volumetric compression, resulting in the formation of cracks and pathways that increase the water absorption rate and consequently decrease the apparent bulk density. A noteworthy observation was the decrease in water absorption as the proportion of pore-forming agents decreased, with some stability observed in $LFA_{30}F$-0.2, and $LFA_{30}F$-0.4 samples.

3.2.4 | Phase evolution after thermal treatment

Figures 9 and 10 present the FTIR and XRD of the sample $LFA_{30}F$-0.7 chosen among others to deeply assess the impact of high temperature on porous laterite-based geopolymer Foam. The choice of the characterized sample was based on the low thermal conductivity and high flexural strength. Figure 9 shows the FTIR spectrum of the same sample before and after exposure at different temperatures. The sample showed a decrease in the intensity of the absorption band related to the stretching mode of the O–H group at 3750 and 1615 cm^{-1} when compared to the spectrum of the initial sample. This indicates the dehydration and dihydroxylation process that occurred upon heating from 25°C to 900°C. During the geopolymerization reaction it was expected the formation amorphous hydrated iron aluminosilicate (such as Fe–N–A–S–H types) from a

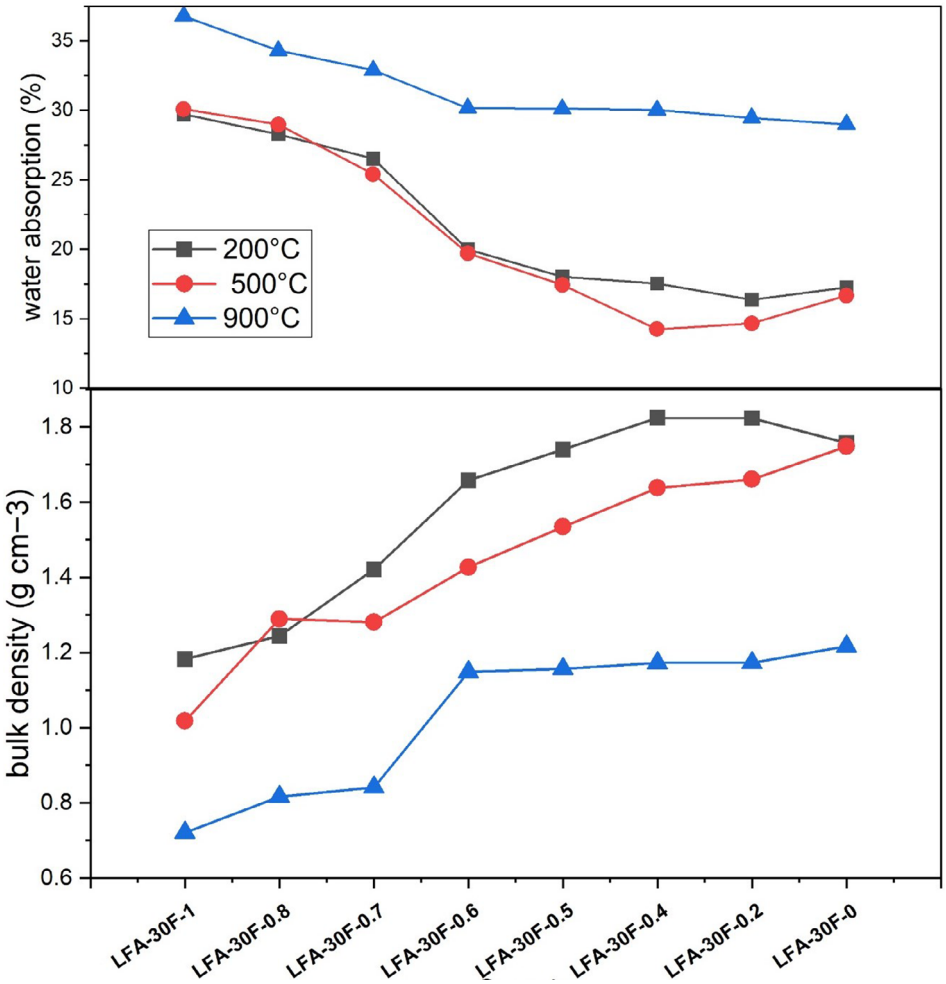

FIGURE 8 Water absorption and apparent porosity after exposure at different temperatures.

mixture of laterite and reactive silica (SiO_2) in contact with an alkaline solution.[6] These gels contain hydroxyl groups linked to aluminium and iron contained in the polymer molecule structure. However, when subjected to a temperature above 200°C, these hydroxyl groups will begin to detach from the structure, but this detachment will be more intense when exposed to a temperature above 900°C. This dihydroxylation of Fe–N–A–S–H gels generates heat release, causing significant linear and volumetric shrinkage in the porous geopolymer matrix. The absorption band at 1480 cm^{-1} shows decarbonation of C–O bonds as the temperature increases. This decrease is due to the reduction of many alkalis in the porous geopolymer, causing the decrystallization of certain crystalline products, which in turn makes the matrix more sensitive to decarbonation.[53] One of the most significant changes occurs in the region between 1000 and 750 cm^{-1}, where a strong change in peak intensity at 900°C was noted, and a slight reduction in peak intensity T–O–T (Al, Fe, Si) between 200°C and 500°C, this reduction may be due to a decrease in the length of the geopolymer chain. This adds value to the results obtained in Section 3.2.1 on the increase in bending strength at 500°C and its fall at 900°C.

The inclusion of iron-rich laterite triggers a glass transition of geopolymers at 900°C, leading to substantial linear shrinkage and densification. Conversely, Rickard et al.[54] demonstrated that the crystallization of fly ash geopolymers could result in thermal expansion and minimal linear shrinkage between 700°C and 800°C. Upon examining the XRD curve post-exposure to 200°C, a characteristic broad bump indicative of N–A–S–H gel (amorphous to semicrystalline sodium aluminosilicates (N–A–S–(H)), similar to samples at 25°C. This aligns with the findings of Kassim and Chern,[55] who noted the appearance of these N–A–S–H gels in the geopolymer paste post-treatment at 200°C. However, with an increase in temperature to 500°C, the disappearance of the diffraction peak at $2\theta = 22.38°$ and 21° was observed, attributed to dihydroxylation and dehydration. Concurrently, the weakening intensity of the quartz peak suggests ongoing polymerization of initially unreacted particles and atomic reorganization, leading to heightened amorphous phase content and improved

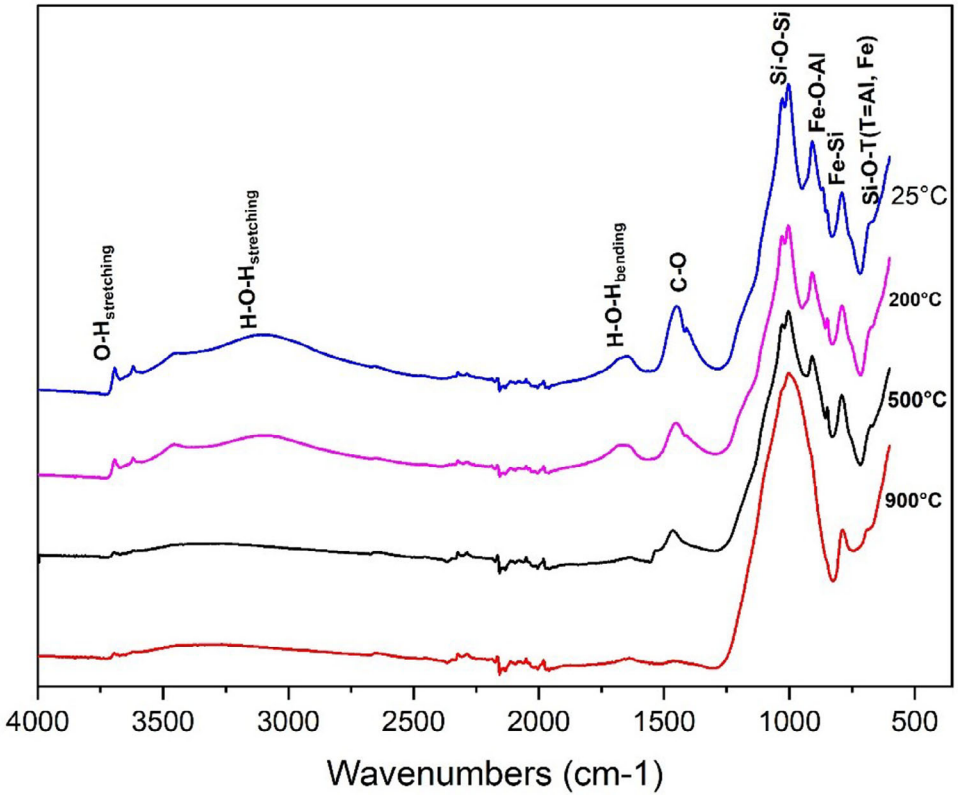

FIGURE 9 Infrared spectra of laterite geopolymers foam (LGF) after exposure at different temperatures.

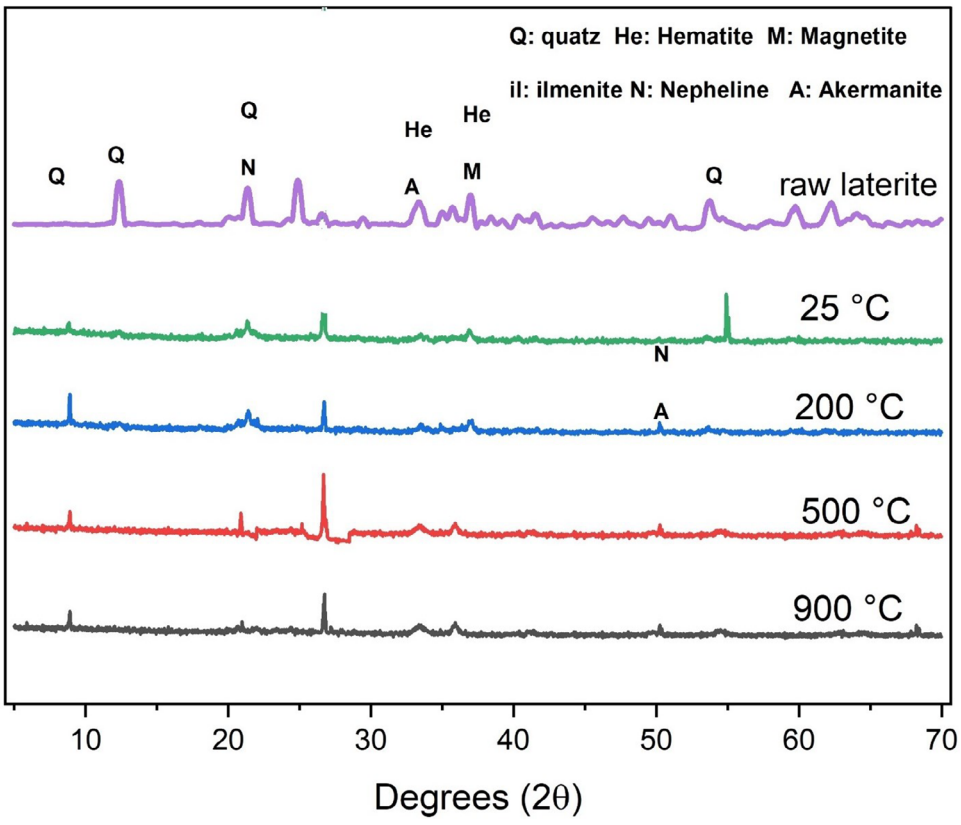

FIGURE 10 X-ray diffraction (XRD) of laterite geopolymers foam (LGF) after exposure at different temperatures.

densification of the porous geopolymer matrix, thereby enhancing mechanical properties at 500°C.

Upon further elevation of temperature to 900°C, notable changes were observed in the XRD curve compared to the raw laterite powder and sample cured at 25°C, notably the emergence of crystalline phases as the amorphous phase gradually diminishes. The expansion of the crystalline phase is considered a primary factor contributing to the development of microcracks and damage in geopolymers post-exposure to 900°C, leading to a decline in flexural or compressive strength.[18] One of the amorphous phases transitioning into a crystalline phase is nepheline ($NaAlSiO_4$). Additionally, observations at elevated temperatures highlighted the formation of an akermanite phase ($Ca_2MgSi_2O_7$) resulting from sintering or associated with devitrification of laterite grains and residual fine aggregates. While XRD data offered a comprehensive explanation for linear shrinkage and flexural resistance, detailed observation of expansion behaviors of crystalline phases was not extensively conducted in this study. In conclusion, it is noteworthy that the presence of iron-rich precursors plays a critical role in the volumetric stabilization of geopolymers under baking conditions. It is essential to recognize that a material's stability under high-temperature conditions is crucial, as high linear shrinkage when exposed to elevated temperatures can lead to structural cracks, collapse, and weakening. This observation underscores the significance of the research conducted by Zhang et al.[16] on the synthesis of geopolymers utilizing fly ash.

4 | CONCLUSION

This study evaluated the thermal insulation, fire resistance, and linear shrinkage of laterite geopolymer foams employing iron-rich laterite and sodium silicate solution as binder precursor, sand as fine aggregate, and aluminium powder as a foaming agent. First, it was discovered that inserting 30% of fine aggregate particles into the porous geopolymer foam enhanced compressive resistance. Second, by keeping this amount fine aggregates while altering the aluminium powder content, changes in mechanical characteristics were found. Laterite geopolymer foam with 0.7% and 0.8% of aluminium powder produced a light and low thermal conductivity (0.10–0.17 W/m K). The foaming agent determines the number and volume of pores, but the alkaline solution plays a major role in pore connectivity. The low thermal conductivity and apparent density of these innovative materials, together with their homogenous pore size distribution, have proved their importance for thermal insulation applications. Furthermore, the results show that high temperature modifies the polymerization step, causing high linear shrinkage and high-volume compression, resulting in matrix cracks and embrittlement, whereas a temperature of 500°C allowed the crystalline network of the porous geopolymers to be reorganized and better arranged.

AUTHOR CONTRIBUTIONS

Conceptualization, data curation, funding acquisition, project administration, resources, visualization, and writing—original draft and editing: Julson Aymard Tchio. *Data interpretation (mercury intrusion porosimetry) and revisions on the manuscript*: Joelle Nadia Nouping Fekoua. *Helped to correct the manuscript of the article*: Cyriaque Rodrigue Kaze, Juho Yliniemi, and Deutou Juvenale. *Funding acquisition, supervision, review, and characterization (XRD, MIP, and FTIR)*: Elie Kamseu. *Helped with supervision and paper revision*: Florence Uphie Chinje and Cristina Leonelli.

ACKNOWLEDGMENTS

This work was supported by the Institut de la Francophonie pour le Développement Durable (IFDD/Canada)/Projet de Déploiement des Technologies et Innovations Environnementales funded by the Organization Internationale de la Francophonie, the Organization of African, Caribbean, and Pacific States, and the European Commission (FED/220/421-370), the Local Materials Promotion Authority (MIPROMALO) of the Ministry of Scientific Research and Innovation of Cameroon who made it possible for this scientific work to be carried out.

CONFLICT OF INTEREST STATEMENT

The authors declare no conflicts of interest.

INFORMED CONSENT

All participants provided informed consent prior to their participation.

ORCID

Julson Aymard Tchio https://orcid.org/0000-0001-6347-608X
Juvenal Giogetti Deuton Nemaleu https://orcid.org/0000-0002-3249-3159
Juho Yliniemi https://orcid.org/0000-0003-0013-8598
Cristina Leonelli https://orcid.org/0000-0001-8524-8715

REFERENCES

1. Lach M. Geopolymer foams—will they ever become a viable alternative to popular insulation materials ?—A critical opinion. Materials. 2021;14:3568.

2. Zhang Z, Provis JL, Reid A, Wang H. Geopolymer foam concrete: an emerging material for sustainable construction. Constr Build Mater. 2014;56:113–27.
3. Bai C, Franchin G, Elsayed H, Zaggia A, Conte L, Li H, et al. High-porosity geopolymer foams with tailored porosity for thermal insulation and wastewater treatment. J Mater Res. 2017;32:3251–59. https://doi.org/10.1557/jmr.2017.127
4. Pola M, Rieger D, Bene J, Pavol Š, Deshmukh K, Kovářík T, et al. Cellular ceramic foam derived from potassium-based geopolymer composite: thermal, mechanical and structural properties. Mater Des. 2021;198:109355. https://doi.org/10.1016/j.matdes.2020.109355
5. Kamseu E, Rodrigue C, Fekoua N, Melo UC, Rossignol S, Leonelli C. Ferrisilicates formation during the geopolymerization of natural Fe-rich aluminosilicate precursors. Mater Chem Phys. 2020;240:122062. https://doi.org/10.1016/j.matchemphys.2019.122062
6. Tchio JA, Yerima N, Kaze CR, Kamseu E, Chinje FU, Leonelli C. Design and characterization of iron–calcium–aluminium–silicate–hydrate as low-temperature binder. Innov Infrastruct Solut. 2024;9:42. https://doi.org/10.1007/s41062-023-01329-w
7. Cui Y, Wang D. Effects of water on pore structure and thermal conductivity of fly ash-based foam geopolymers. Adv Mater Sci Eng. 2019;2019:1–10.
8. Mehta A, Siddique R. An overview of geopolymers derived from industrial by-products. Constr Build Mater. 2016;127:183–98.
9. Nodehi M. A comparative review on foam-based versus lightweight aggregate-based alkali-activated materials and geopolymer. Innov Infrastruct Solut. 2021;6(4):1–20. https://doi.org/10.1007/s41062-021-00595-w
10. Bai C, Li H, Bernardo E, Colombo P. Waste-to-resource preparation of glass-containing foams from geopolymers. Ceram Int. 2019;45:7196–202.
11. Husainie SM, Deng X, Ghalia MA, Robinson J, Naguib HE. Natural fillers as reinforcement for closed-molded polyurethane foam plaques: mechanical, morphological, and thermal properties. Mater Today Commun. 2021;27:102187.
12. Walbrück K, Drewler L, Witzleben S, Stephan D. Factors influencing thermal conductivity and compressive strength of natural fiber-reinforced geopolymer foams. Open Ceram. 2021;5:100065.
13. Abbas AM, Sultan ME, Khater HM, El-Razik MMA, El-Nawawy MA, Sayed AZ. Study physicochemical and thermal properties of eco-friendly lightweight geopolymers incorporating silica sand flour. Arab J Sci Eng. 2023;48:7571–85.
14. Dhasindrakrishna K, Pasupathy K, Ramakrishnan S, Sanjayan J. Progress, current thinking and challenges in geopolymer foam concrete technology. Cem Concr Compos. 2021;116:103886.
15. Abdellatief M, Abd M, Hani E, Aref A, Ahmed AA. A state-of-the-art review on geopolymer foam concrete with solid waste materials: components, characteristics, and microstructure. Innov Infrastruct Solut. 2023;8(9):1–26. https://doi.org/10.1007/s41062-023-01202-w
16. Zhang X, Bai C, Qiao Y, Wang X, Jia D, Li H, et al. Porous geopolymer composites: a review. Compos Part A. 2021;150:106629. https://doi.org/10.1016/j.compositesa.2021.106629
17. Novais RM, Pullar RC, Labrincha JA. Geopolymer foams: an overview of recent advancements. Prog Mater Sci. 2020;109:100621. https://doi.org/10.1016/j.pmatsci.2019.100621
18. Le VS, Szczypinski MM, Hájková P, Kovacic V, Bakalova T, Volesky L, et al. Mechanical properties of geopolymer foam at high temperature. Sci Eng Compos Mater. 2020;27:129–38.
19. Ain N, Yun-Ming L, Cheng-Yong H, Mustafa M, Bakri A. Correlation between pore structure, compressive strength and thermal conductivity of porous metakaolin geopolymer. Constr Build Mater. 2020;247:118641. https://doi.org/10.1016/j.conbuildmat.2020.118641
20. Szabó R, Mucsi G. Generally about geopolymer foams. Inst Raw Mater Prep Environ Process. 2015:1–6. https://doi.org/10.26649/musci.2015.01
21. Vaou V, Panias D. Thermal insulating foamy geopolymers from perlite. Miner Eng. 2010;23(14):1146–51. https://doi.org/10.1016/j.mineng.2010.07.015
22. Kamseu E, Ngouloure ZNM, Ali BN, Valentini L, Sylvie SZ. Pore network and microstructure in the prediction of heat flux transport in sponge-like geopolymers for thermal insulation. J Therm Anal Calorim. 2022;147:12329–44. https://doi.org/10.1007/s10973-022-11396-3
23. Kočí V, Černý R. Directly foamed geopolymers: a review of recent studies. Cem Concr Compos. 2022;130:104530. https://doi.org/10.1016/j.cemconcomp.2022.104530
24. Łach M, Mikuła J, Lin WT, Bazan P, Figiela B, Korniejenko K. Development and characterization of thermal insulation geopolymer foams based on fly ash. Proc Eng Technol Innov. 2020;16:23–29.
25. Batool F, Rafi MM, Bindiganavile V. Microstructure and thermal conductivity of cement-based foam: a review. J Build Eng. 2018;20:696–704. https://doi.org/10.1016/j.jobe.2018.09.008
26. Ngouloure ZNM, Kamseu E, Moungam LMB, Tchakoute HK, Valentini L, Leonelli C. Design of porous geopolymers for hygrothermal applications: role of nano and meso porosity. Silicon. 2022;14:10045–59. https://doi.org/10.1007/s12633-022-01741-4
27. Zhang Z, Provis JL, Reid A, Wang H. Mechanical, thermal insulation, thermal resistance and acoustic absorption properties of geopolymer foam concrete (GFC). Cem Concr Compos. 2015;62:97–105. https://doi.org/10.1016/j.cemconcomp.2015.03.013
28. Kaze RC, Moungam LMB, Djouka MLF, Nana A, Kamseu E, Melo UFC, et al. Applied clay science the corrosion of kaolinite by iron minerals and the effects on geopolymerization. Appl Clay Sci. 2017;138:48–62. https://doi.org/10.1016/j.clay.2016.12.040
29. Ibrahim WMW, Ahmad R, Coman BT, Abdullah MMAB, Puskas A, Jaganathan VS. The effects of solid to liquid ratio on fly ash based lightweight geopolymer. IOP Conf Ser Mater Sci Eng. 2020;877:012013. https://doi.org/10.1088/1757-899X/877/1/012013
30. Arrasi K. Metakaolin geopolymer foam using aluminium powder. Int J Emerg Technol Adv Eng. 2019.
31. Beghoura I, Castro-Gomes J. Design of alkali-activated aluminium powder foamed materials for precursors with different particle sizes. Constr Build Mater. 2019;224:682–90. https://doi.org/10.1016/j.conbuildmat.2019.07.018
32. Ducman V, Korat L. Materials characterization of geopolymer fly-ash based foams obtained with the addition of Al powder or

H_2O_2 as foaming agents. Mater Charact. 2016;113:207–13. https://doi.org/10.1016/j.matchar.2016.01.019

33. Korniejenko K, Miku J. Thermal insulation and thermally resistant materials made of geopolymer foams. Proc Eng. 2016;151:410–16. https://doi.org/10.1016/j.proeng.2016.07.350
34. Radina L, Sprince A, Pakrastins L, Gailitis R, Sakale G. Mechanical strength and microstructure of metakaolin/volcanic ash-based geopolymer composites reinforced with reactive silica from rice husk ash (RHA). J Phys Conf Ser. 2023;2423:012032. https://doi.org/10.1088/1742-6596/2423/1/012032
35. Vadivelu K, Aravind R, Dani DPJJ, Basha CSA, Basilahamed S. Strength assessment of lightweight geopolymer wall panels infilled with expanded polystyrene. Int J Innov Res Technol. 2019;5(11):111–15.
36. Liu YL, Liu C, Qian LP, Wang AG, Sun DS, Guo D. Foaming processes and properties of geopolymer foam concrete: effect of the activator. Constr Build Mater. 2023;391:131830.
37. Masi G, Rickard WDA, Vickers L, Chiara M, RA Van. A comparison between different foaming methods for the synthesis of light weight geopolymers. Ceram Int. 2014;40(9):13891–902. https://doi.org/10.1016/j.ceramint.2014.05.108
38. Yan S, Ren X, He C, Wang W, Zhang M, Xing P. Microstructure evolution and properties of red mud/slag-based cenosphere/geopolymer foam exposed to high temperatures. Ceram Int. 2023;49:34362–74.
39. Novais RM, Ascensão G, Ferreira N, Seabra MP, Labrincha JA. Influence of water and aluminium powder content on the properties of waste-containing geopolymer foams. Ceram Int. 2018;44:6242–49.
40. Xu F, Gu G, Zhang W, Wang H, Huang X, Zhu J. Pore structure analysis and properties evaluations of fly ash-based geopolymer foams by chemical foaming method. Ceram Int. 2018;44(16):19989–97. https://doi.org/10.1016/j.ceramint.2018.07.267
41. Bai C, Zheng J, Rizzi GA, Colombo P. Low-temperature fabrication of SiC/geopolymer cellular composites. Compos Part B: Eng. 2018;137:23–30. https://doi.org/10.1016/j.compositesb.2017.11.013
42. Wu J, Zhang Z, Zhang Y, Li D. Preparation and characterization of ultra-lightweight foamed geopolymer (UFG) based on fly ash-metakaolin blends. Constr Build Mater. 2018;168:771–79.
43. Krzywon R, Dawczyński S. Strength parameters of foamed geopolymer reinforced with GFRP mesh. Materials. 2021;14:689.
44. Le VS, Nguyen VV, Sharko A, Ercoli R, Nguyen TX, Tran DH, et al. Fire resistance of geopolymer foams layered on polystyrene boards. Polymers (Basel). 2022;14(10):1945. https://doi.org/10.3390/polym14101945
45. Kong DLY, Sanjayan JG, Sagoe-Crentsil K. Comparative performance of geopolymers made with metakaolin and fly ash after exposure to elevated temperatures. Cem Concr Res. 2007;37:1583–89. https://doi.org/10.1016/j.cemconres.2007.08.021
46. He R, Dai N, Wang Z. Thermal and mechanical properties of geopolymers exposed to high temperature: a literature review. Adv Civil Eng. 2020.
47. Sarazin J, Davy CA, Bourbigot S, Tricot G, Hosdez J, Lambertin D, et al. Flame resistance of geopolymer foam coatings for the fire protection of steel. Compos Part B. 2021;222:109045. https://doi.org/10.1016/j.compositesb.2021.109045
48. Peng X, Li H, Shuai Q, Wang L. Fire resistance of alkali activated geopolymer foams produced from metakaolin and Na_2O_2. Materials. 2020;13:535. https://doi.org/10.3390/ma13030535
49. Kuenzel C, Vandeperre LJ, Donatello S, Boccaccini AR, Cheeseman C. Ambient temperature drying shrinkage and cracking in metakaolin-based geopolymers. J Am Ceram Soc. 2012;3277:3270–77. https://doi.org/10.1111/j.1551-2916.2012.05380.x
50. Cheng-Yong H, Yun-Ming L, Al Bakri, Abdullah MM, Hussin K. Thermal resistance variations of fly ash geopolymers: foaming responses. Sci Rep. 2017;7:45355. https://doi.org/10.1038/srep45355
51. Provis JL, Harrex RM, Bernal SA, Duxson P, van Deventer JSJ. Dilatometry of geopolymers as a means of selecting desirable fly ash sources. J Non Cryst Solids. 2012;358(16):1930–37. https://doi.org/10.1016/j.jnoncrysol.2012.06.001
52. Huang Y, Gong L, Shi L, Cao W, Pan Y, Cheng X. Experimental investigation on the influencing factors of preparing porous fly ash-based geopolymer for insulation material. Energy Build. 2018;168:9–18.
53. Kassem NN, Ahmed DA, Kishar EA. Effect of elevated temperatures on the performance of metakaolin geopolymer pastes incorporated by cement kiln dust. Egypt J Chem. 2021;64:1911–26. doi: 10.21608/EJCHEM.2021.50848.3041
54. Rickard WDA, van Riessen A, Walls P. Thermal character of geopolymers synthesized from class F fly ash containing high concentrations of iron and α-quartz. Int J Appl Ceram Technol. 2010;7(1):81–88. https://doi.org/10.1111/j.1744-7402.2008.02328.x
55. Kassim KA, Chern KK. The soil samples were chosen to represent plasticity index ranging from 20. 2004;16(1):13–23.

How to cite this article: Tchio JA, Fekoua JNN, Kaze CR, Nemaleu JGD, Yliniemi J, Kamseu E, et al. Improving thermal insulation and thermal resistance properties of laterite-based geopolymer foams by direct foaming. Int J Appl Ceram Technol. 2025;22:e14959. https://doi.org/10.1111/ijac.14959